



LIGO Laboratory / LIGO Scientific Collaboration

LIGO-T010074-03-D

07/17/2001

The LIGO Observatory Environment

LIGO Systems, Ed. D. Shoemaker

Distribution of this document:
LIGO Science Collaboration

This is an internal working note
of the LIGO Project.

California Institute of Technology
LIGO Project – MS 18-34
1200 E. California Blvd.
Pasadena, CA 91125
Phone (626) 395-2129
Fax (626) 304-9834
E-mail: info@ligo.caltech.edu

Massachusetts Institute of Technology
LIGO Project – NW17-161
175 Albany St
Cambridge, MA 02139
Phone (617) 253-4824
Fax (617) 253-7014
E-mail: info@ligo.mit.edu

LIGO Hanford Observatory
P.O. Box 1970
Mail Stop S9-02
Richland WA 99352
Phone 509-372-8106
Fax 509-372-8137

LIGO Livingston Observatory
P.O. Box 940
Livingston, LA 70754
Phone 225-686-3100
Fax 225-686-7189

<http://www.ligo.caltech.edu/>

Table of Contents

1	<i>Introduction</i>	4
1.0	Document plan and evolution	4
1.1	Purpose	4
1.2	Scope	4
1.3	Definitions	4
1.4	Acronyms	4
1.5	Applicable Documents	5
1.5.1	LIGO Documents	5
1.5.2	Non-LIGO Documents.....	5
2	<i>Seismic environment</i>	6
2.0	Standard design data for the two sites	6
2.0.1	Spectra.....	6
2.1	Livingston	7
2.1.1	Spectra, variability	7
2.1.2	RMS levels	8
2.1.3	Histograms for low frequencies	10
2.1.4	Newtonian background	12
2.1.5	Earthquakes	12
2.1.6	Impulsive motion	12
2.1.7	Identified sources, additional information	12
2.2	Hanford	13
2.2.1	Spectra, variability	13
2.2.2	RMS Levels.....	18
2.2.3	Newtonian background	20
2.2.4	Earthquakes	21
2.2.5	Impulsive motion	22
2.2.6	Identified sources, additional information	23
3	<i>Acoustic environment</i>	25
3.1	Livingston	25
3.1.1	Spectra, variability	25
3.1.2	Impulsive events.....	25
3.1.3	Identified sources, additional information	25
3.2	Hanford	25
3.2.1	Spectra, variability	25
3.2.2	Impulsive events.....	26
3.2.3	Identified sources, additional information	26
4	<i>Electromagnetic environment</i>	27
4.1	Livingston	27

4.1.1	Spectra, variability	27
4.1.2	Impulsive events.....	28
4.1.3	Identified sources, additional information	28
4.2	Hanford.....	28
4.2.1	Spectra, variability	28
4.2.2	Impulsive events.....	30
4.2.3	Identified sources, additional information	30
5	<i>Thermal and barometric environment</i>	31
5.1	Livingston.....	31
5.2	Hanford	31
6	<i>Vacuum environment.....</i>	34
6.1	Livingston.....	35
6.2	Hanford	35

1 Introduction

1.0 Document plan and evolution

This document should serve as a ready and up-to-date reference for design and sanity checks. For this to be true, it must

- Consist of standard plots for similar measurements at different times and places and between sites
- Give pointers to data for the plots to allow quantitative analysis, and give fits and approximations for estimates
- Be updated regularly to indicate the latest information on the measured quantities

The current draft is a start at canvassing the available data (it is certain that the report is missing a lot of existing relevant data) and looking for the right means to organize and present those data. Comments to David Shoemaker (dhs@ligo.mit.edu) are invited.

1.1 Purpose

This document gives an overview of the environment at the LIGO sites relevant to the design and operation of the instruments, and provides pointers to additional sources of information. The document is organized by the quantity measured, dealing first with one site (LLO) and then the other (LHO).

1.2 Scope

The scope of this document covers those aspects of the environment which directly relate to the instrument design and performance. The scope does not include aspects that relate to installation of detector components or maintenance of the physical plant, for instance the outside temperature, the humidity of the air in the LVEA or dust in the LVEA. These latter issues, and acceptable materials and processes for detector fabrication are covered in ‘Generic Requirements for Detector Subsystems’, E010123-00.

A general description of the PEM components used for the measurements can be found in the PEM Final Design document.

1.3 Definitions

TBD

1.4 Acronyms

See http://www.ligo.caltech.edu/LIGO_web/docs/acronyms.html

1.5 Applicable Documents

1.5.1 LIGO Documents

Document Number	Title
T010075-00-D	Advanced LIGO Systems Design
E010123-00	Generic Requirements for Detector Subsystems
G000262-00	Source and propagation...
T010070-00-D	First look at using Streckeisen STS-2 seismometer signals to predict LIGO arm length control signals.
T010073-00-L	Geophysical Measurements Along the X Arm at LLO
E990303-03-D	Seismic Isolation Subsystem Design Requirements Document
	E. Daw 28 June 2001 email
T970112	PEM (Physics Environmental Monitoring) Final Design
	S. Chatterji 16 May 2001 email

1.5.2 Non-LIGO Documents

- USGS earthquake information <http://geohazards.cr.usgs.gov/eq/>
- Seismic gravity-gradient noise in interferometric gravitational-wave detectors, Hughes and Thorne, Physical Review D 58 1220002

2 Seismic environment

2.0 Standard design data for the two sites

2.0.1 Spectra

To aid in initial design efforts and to summarize the data, a fit [E990303-03-D] to the seismic noise for the two sites has been made; this is shown in Figure 1.

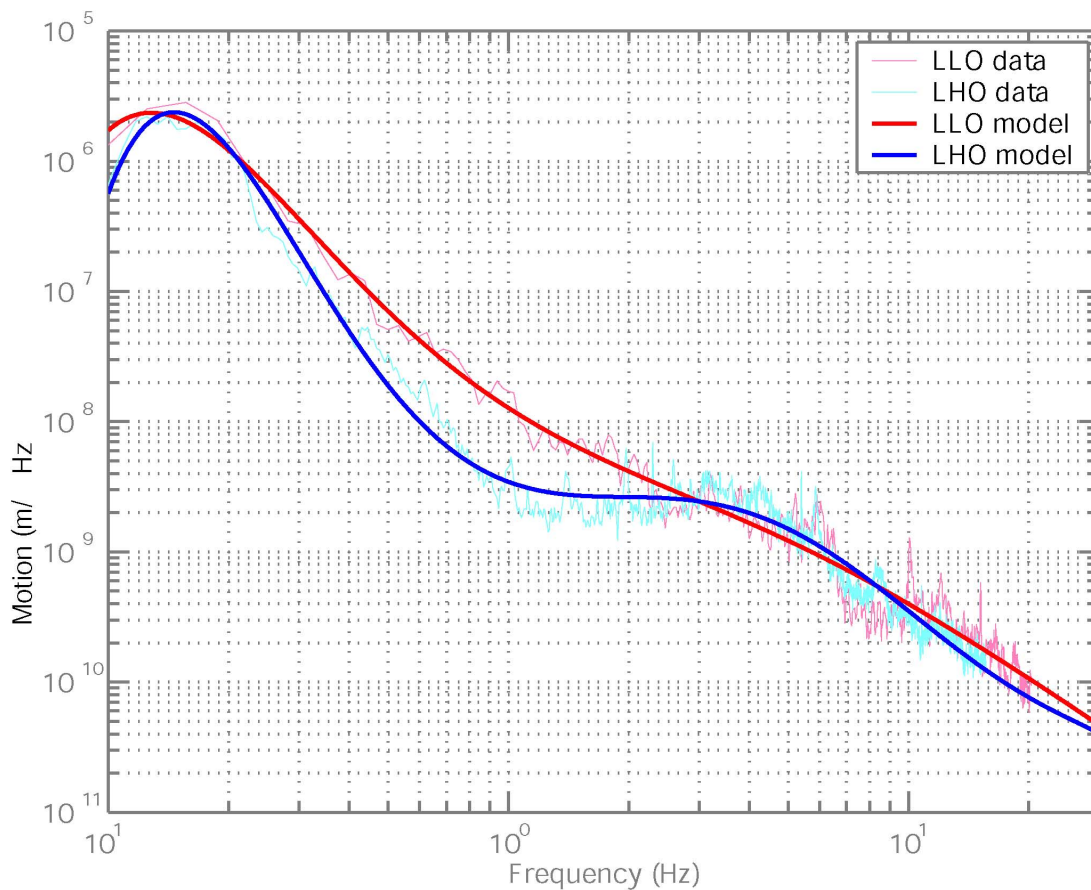


Figure 1: Polynomial fit to ‘normal’ seismic data

Because the average ground noise at the two observatories differ significantly, two separate ground noise models are carried for LHO and LLO. This rough description in Figure 1 assumes that all three translational degrees-of-freedom are the same; this is not perfectly correct, but a reasonable starting point.

The ground noise models shown in Figure are polynomial fits in log-space:

$$\log x_g(f) = p_1(\log f)^n + p_2(\log f)^{n-1} + \dots + p_n(\log f) + p_{n+1}$$

where $x_g(f)$ is the displacement spectral density at frequency f . The coefficients are:

LHO: [-0.2889, -0.2406, 3.3449, -2.8481, -3.5256, 3.7009, -1.1333, -8.4617]

LLO: [-0.2428, 0.9749, -0.9445, -0.8139, 1.5001, -1.9789, -7.8940]

The fit is valid over the interval $0.1 < f < 40$ Hz, although it must be stressed that the data may not be valid for frequencies lower than ~ 0.5 Hz due to noise in the seismometers.

Plan: Seismometers with better sensitivity (rejection of temperature fluctuations) at low frequencies will soon be implemented to re-measure and a new ‘average’ spectrum will be fit.

2.1 Livingston

2.1.1 Spectra, variability

In the low-frequency to mid-frequency, data were taken during the E4 run (13 May 2001).

Streckeisen STS-2 signals during L4 run

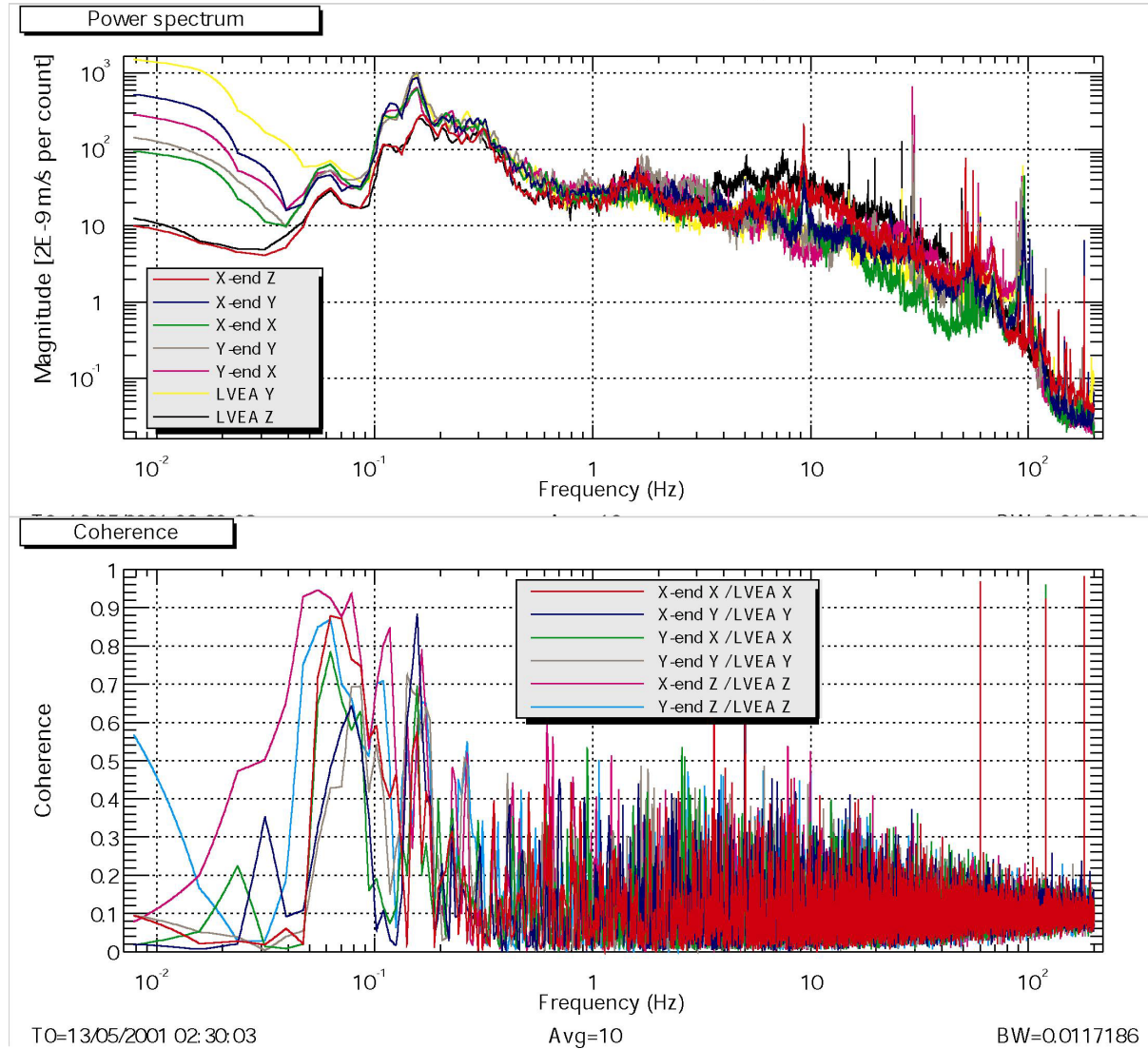


Figure 2: LLO seismic velocity spectra and coherence, 13 May 2001 [Giame/LSU]

2.1.2 RMS levels

Band-limited RMS channels for the Guralp seismometers for a typical Saturday (no construction, but with some daytime traffic) is shown in Figure 3.

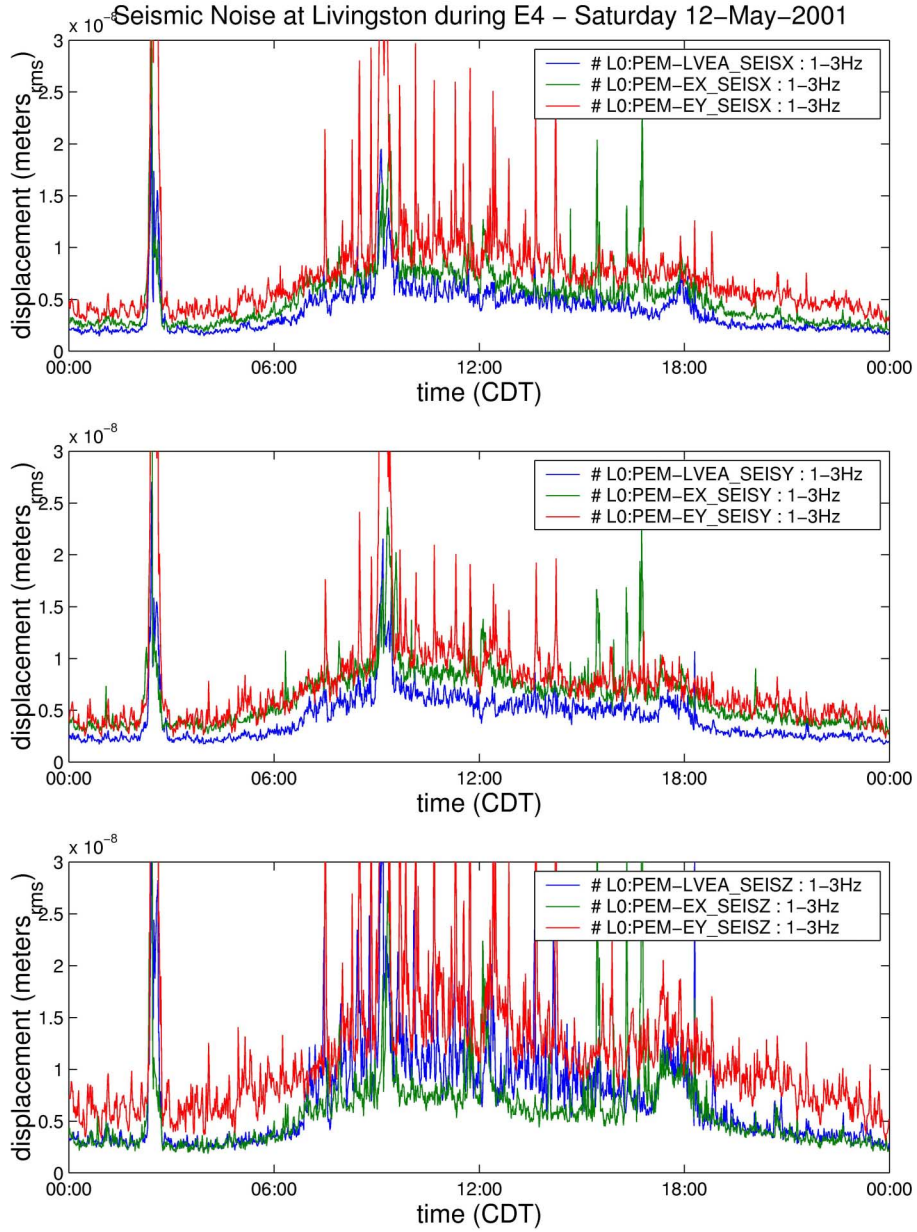


Figure 3: Band-limited RMS, LLO [Johnson/LSU]

2.1.3 Histograms for low frequencies

At low frequencies (below 10 Hz), there are considerable differences between the two sites in the spectrum and its stationarity. Measurements [Daw] have been performed and analyzed as a histogram of bins, with each point representing a one-minute time interval; see Figure 4 for an example.

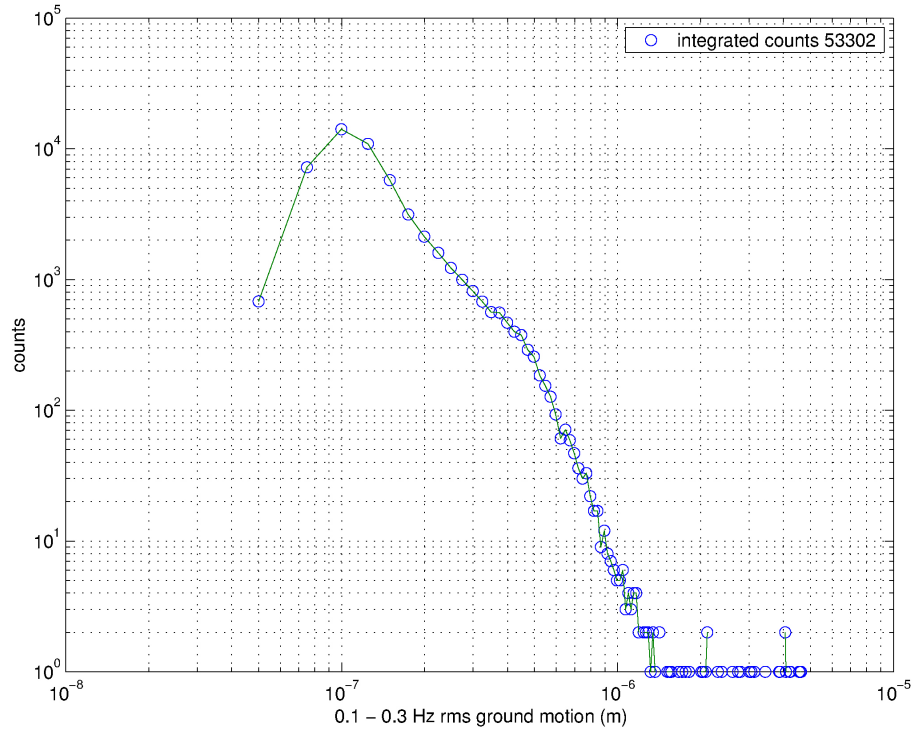


Figure 4: Histogram of low-frequency (principally micro-)seismic activity at LLO May 15 - June 22 2001 [Daw/LSU]

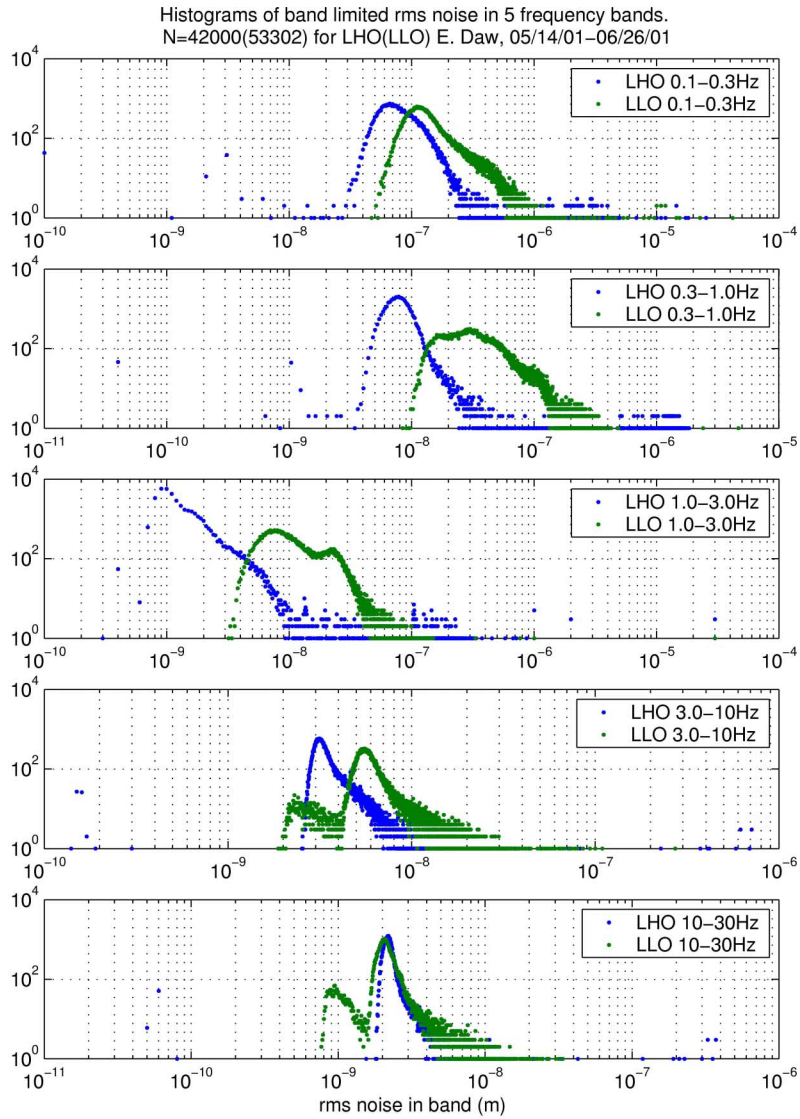


Figure 5: Histograms from LLO and LHO in a range of frequency bins. [Daw/LSU]

Figure 5 shows a much broader range of data. There were 42000 samples, each 1 minute long for the Hanford data set and 53302 for the Livingston data set. The vertical and horizontal scales are the same for the two sites. Note that histogram bins are linear spaced, but the histogram is plotted on a log scale. This means that a higher blue peak further over to the left may actually contain less events than a less high green peak over to the right, since the green dots making up the green peak are more densely packed.

2.1.4 Newtonian background

2.1.5 Earthquakes

The Livingston observatory lies at 30.563 in Latitude, -90.774 in Longitude. The USGS estimates the probability to exceed a certain acceleration in a 50 yr span to be as follows:

Probability of exceedance in 50 Yr	Peak ground acceleration, %g
10%	1.8%
5%	3.4%
2%	6.7%

Table 1: Earthquake acceleration probabilities, LLO

2.1.6 Impulsive motion

2.1.7 Identified sources, additional information

2.1.7.1 Geophysical Measurements Along the X Arm at LLO

Measurements [T010073-00-L] of the velocity of sound for the compressional and vertical shear modes of propagation along the X-arm were made using an impulsive seismic source. The compressional wave propagation velocity is 1780 ± 80 m/sec and is independent of frequency in the 22-34 Hz region. The vertical shear wave propagation velocity varies from 230-440 meters/second over the frequency region from 4-16 Hz. The vertical shear wave mode loss quality factor, Q , varies from about 3-14 over this frequency interval. The compressional wave mode Q values vary from 3-70 over the frequency interval from 22-34 Hz. The mean values of the $1/e$ attenuation lengths for the time domain signals are 300 ± 6 meters for the vertical shear mode and about 1540 ± 50 meters for the compressional wave mode. The Poisson ratio is roughly estimated to be about 0.48. The X-arm of the interferometer appears to act as a seismic waveguide with compressional wave cutoff frequency around 20 Hz.

2.2 Hanford

2.2.1 Spectra, variability

2.2.1.1 Seismometer measurements

Measurements [Schofield] with the Guralp seismometers have been made which represent ‘normal’ operating conditions (during engineering runs).

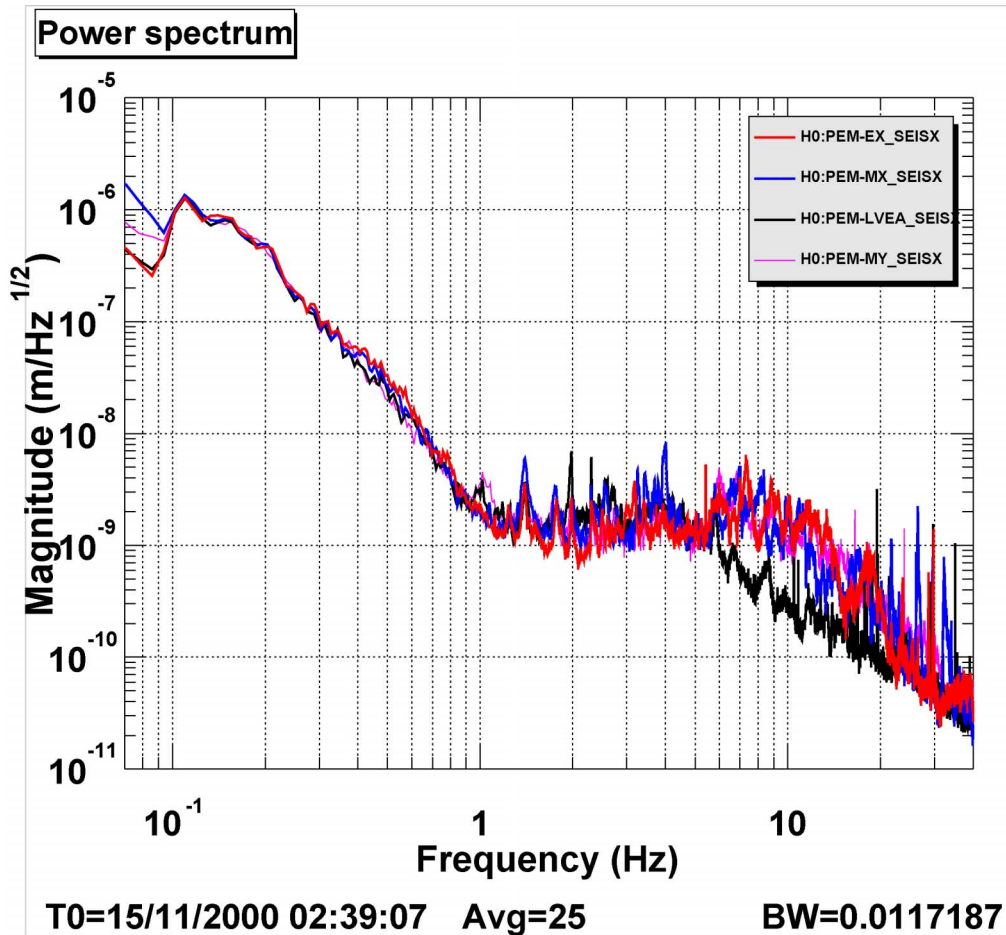


Figure 6: LHO Seismic spectra, 'x' direction

<http://blue.ligo-wa.caltech.edu/users/robert/samplespectra/allseis.xml>

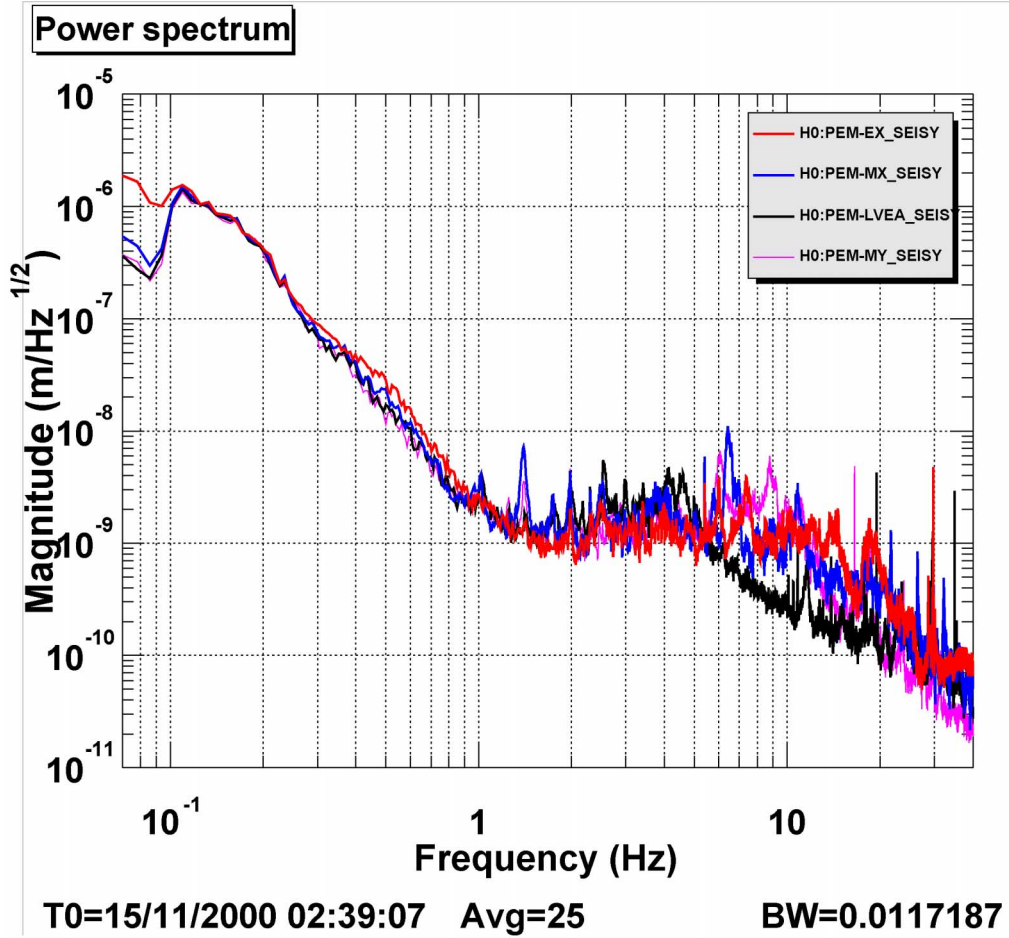


Figure 7: LHO Seismic motion, 'y' direction

<http://blue.ligo-wa.caltech.edu/users/robert/samplespectra/allseis.xml>

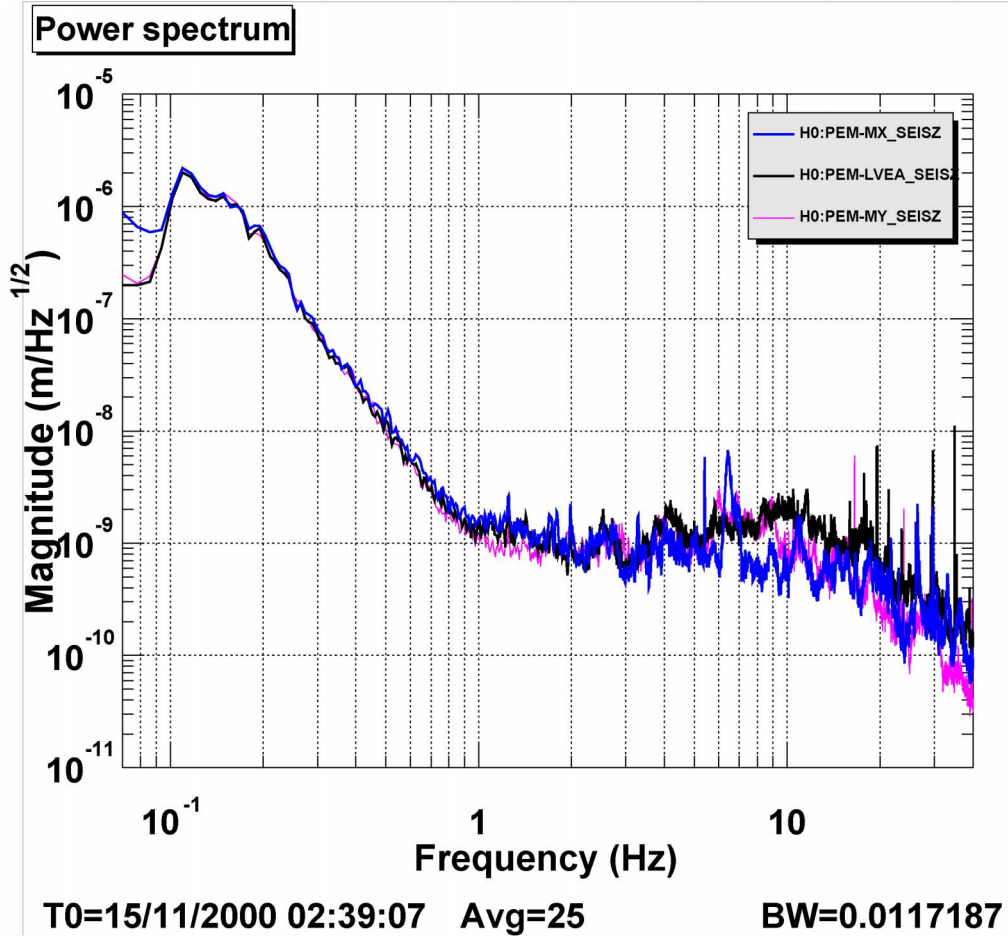


Figure 8: LHO Seismic motion, 'z' direction:

<http://blue.ligo-wa.caltech.edu/users/robert/samplespectra/allseis.xml>

Some examples of noisy seismic activity for LHO are shown in Figure 9. Truck signals of the plotted magnitude appear several times an hour during the day and drop to about once per hour during the night. The signals remain at nearly the plotted level for a few minutes as the trucks pass. Wind velocity reached or exceeded 14 m/s during 4% of the hours in the year-long data set shown in Figure 22. Wind velocities reached or exceeded 7.5 m/s during 28% of the hours in the year.

Seismically Noisy Periods at Hanford

Below 0.1 Hz, signal probably indicates tilt, not displacement.

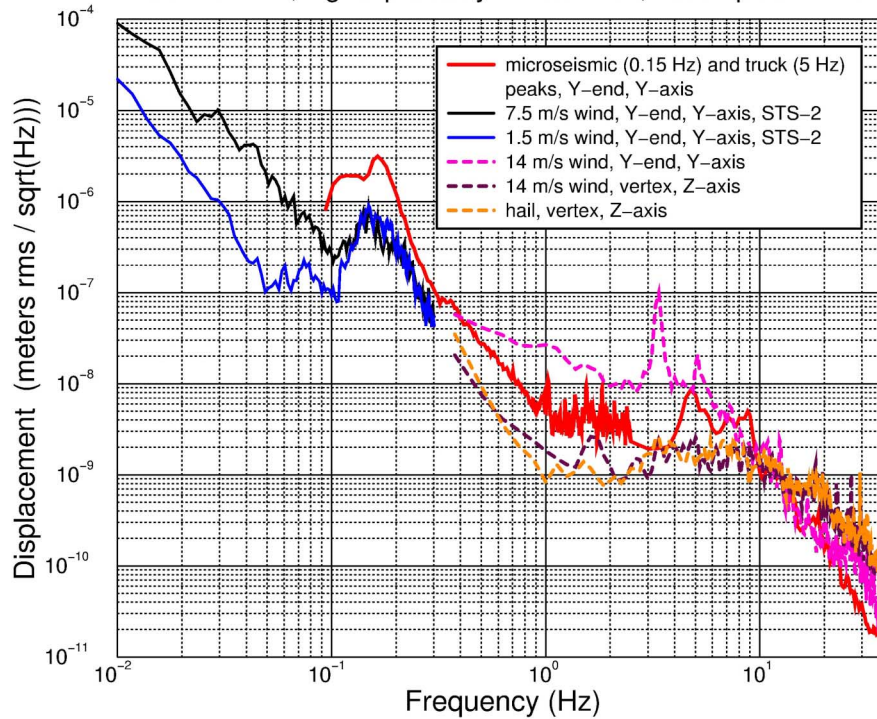


Figure 9: Seismically noisy periods, LHO [Schofield]

2.2.1.2 Accelerometer measurements

Accelerometers mounted on the seismic support tubes monitor the motion with some dynamics from the support piers and seismic isolation system. The piers and the support tubes are part of the infrastructure, common for initial LIGO and the design for Advanced LIGO, although the load on the support tubes (the isolation stack) dynamics and mass will be different for Adv LIGO.

Sample spectra are shown in Figure 10.

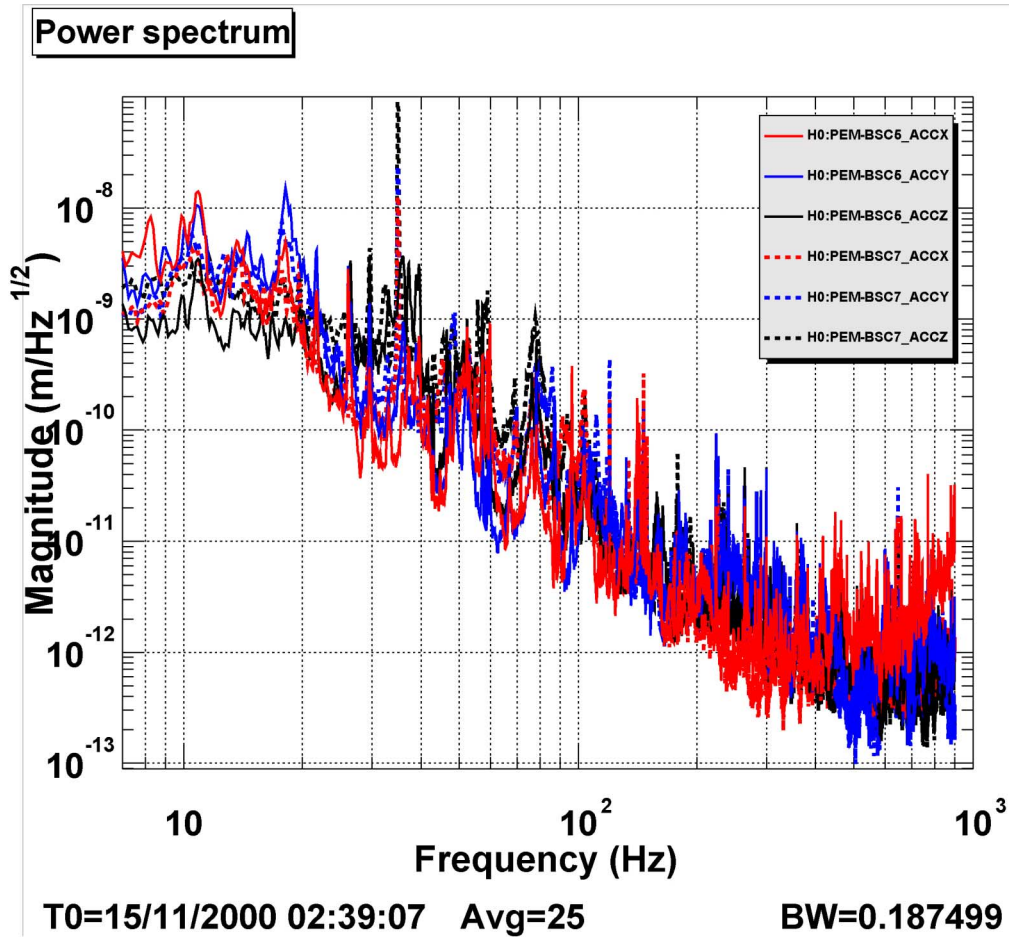


Figure 10: Accelerometers mounted on seismic support tubes

<http://blue.ligo-wa.caltech.edu/users/robert/samplespectra/allaccel.xml>

Sample spectra are shown in Figure 10. BSC5 is located at the Mid-X station, BSC7 is located in the LVEA.

A comparison with the seismometers, Figure 11, makes the increase above the ground motion more evident.

Figure 11 is a comparison (at a different time) between accelerometers and seismometers,

and makes the increase above

the ground motion more evident. Broken lines show accelerometers; BSCs

7 and 8 are in the LVEA.

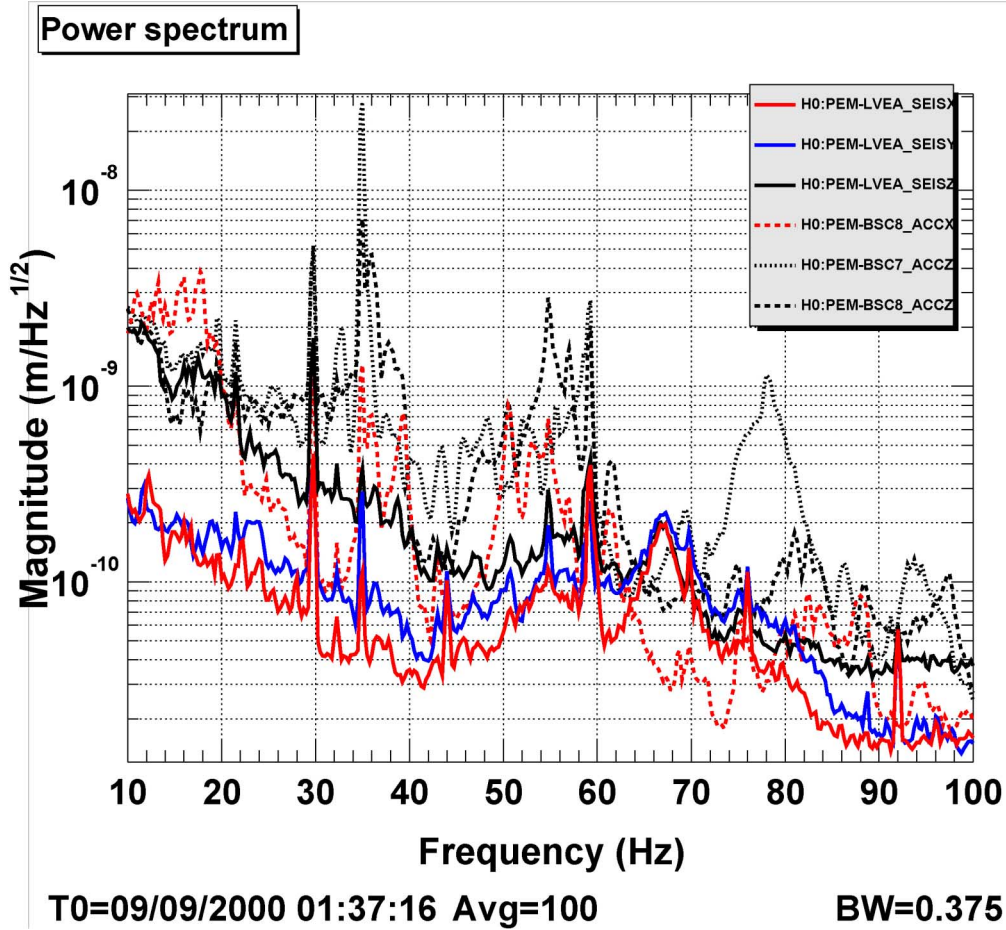


Figure 11: Accelerometers (on Seismic support tubes) and seismometer signals
<http://blue.ligo-wa.caltech.edu/users/robert/samplespectra/accelseis.xml>

2.2.2 RMS Levels

Band-limited RMS channels for the Guralp seismometers for a typical Saturday (no construction, but with some daytime traffic) is shown in Figure 12; compare with Figure 3 for LLO (same time, same scale).

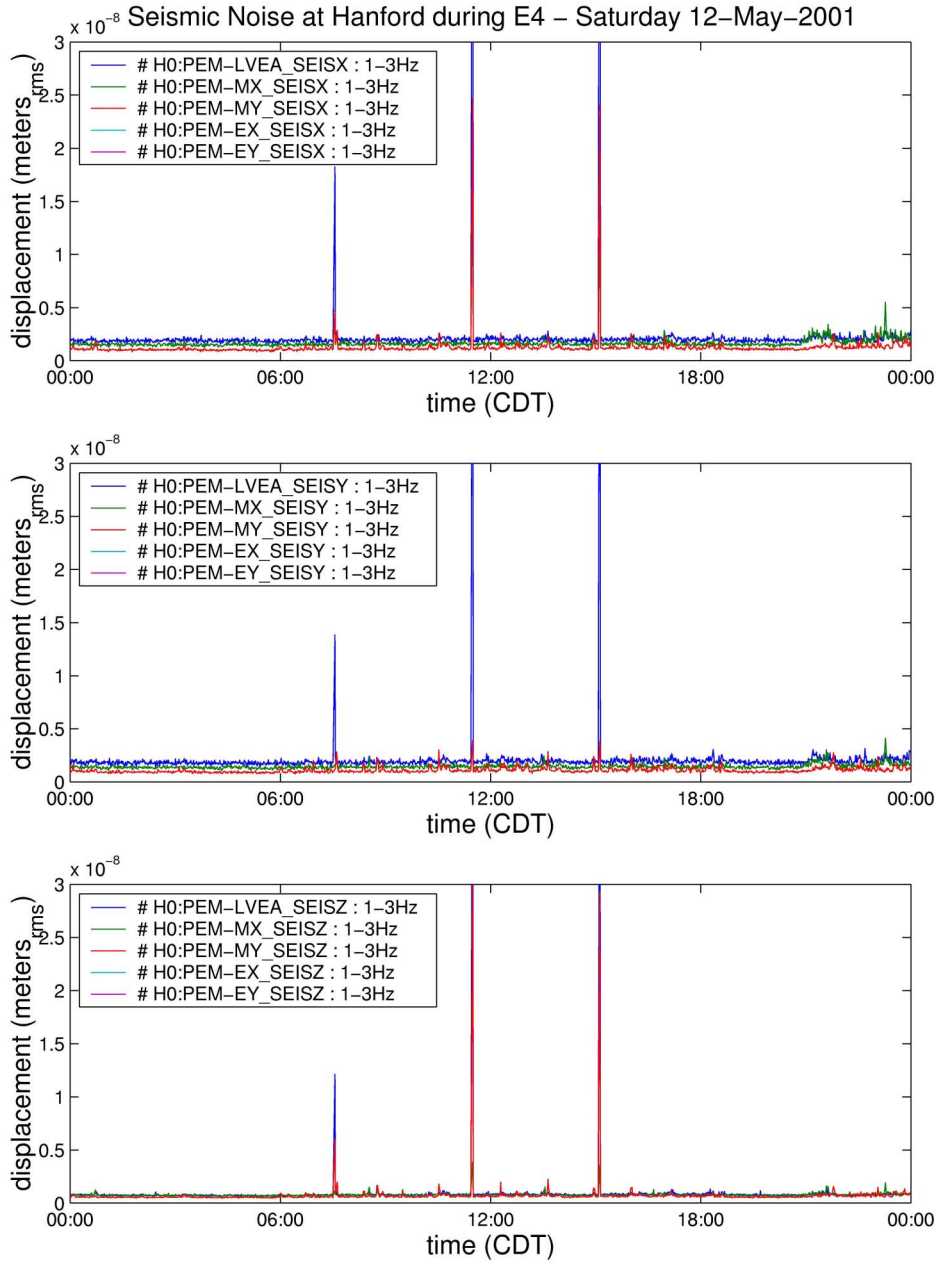


Figure 12: RMS seismic levels, LHO [Schofield/Johnson]

2.2.3 Newtonian background

The Newtonian (or gravity gradient) background has been estimated by Saulson, and more recently by Hughes and Thorne. Subsequently, Schofield has made some measurements of the propagation characteristics of the ground at Hanford, and measurements of the ground noise. His rough estimates, subject to further measurements and analysis, are shown ‘on top of’ the curves from the Hughes and Thorne paper.

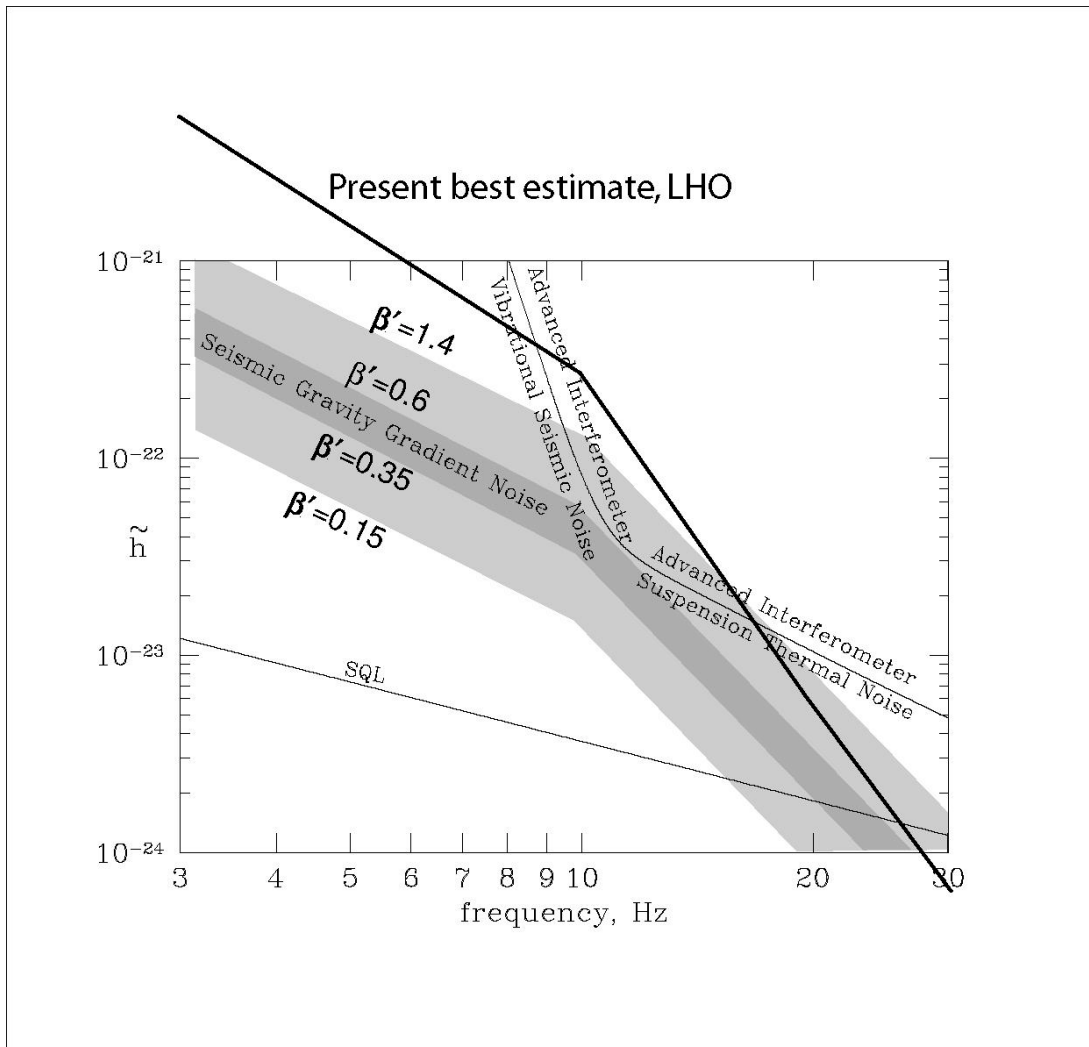


Figure 13: Newtonian background estimate, LHO. The ‘Advanced Interferometer’ curve is not from our present Advanced LIGO design (but it not far from the mechanical limits to sensitivity) [Schofield]

The points at 3 and 10 Hz are based on typical truck traffic excitation at Yend station, anisotropy ratio of 1, and an assumption of RF and Love modes (propagation velocity of 450 m/sec). The points at 20 and 30 Hz are based on measurements in the LVEA with only minimum equipment operating (no 4k racks at that time), an assumed an RF mode.

2.2.4 Earthquakes

Hanford lies at 46.4551 Latitude, -119.4075 Longitude. The USGS estimates the probability to exceed a certain acceleration in a 50 yr span to be as follows:

Probability of exceedance in 50 Yr	Peak ground acceleration, %g
10%	8.5%
5%	12.3%
2%	19.4%

Table 2: Earthquake acceleration probabilities, LHO

Data from the Olympia Earthquake of 28 Feb 2001 are shown in Figure 14 and the one following. The peak of the motion lies close to 0.7 Hz (unfortunate for the initial LIGO pendulum frequency).

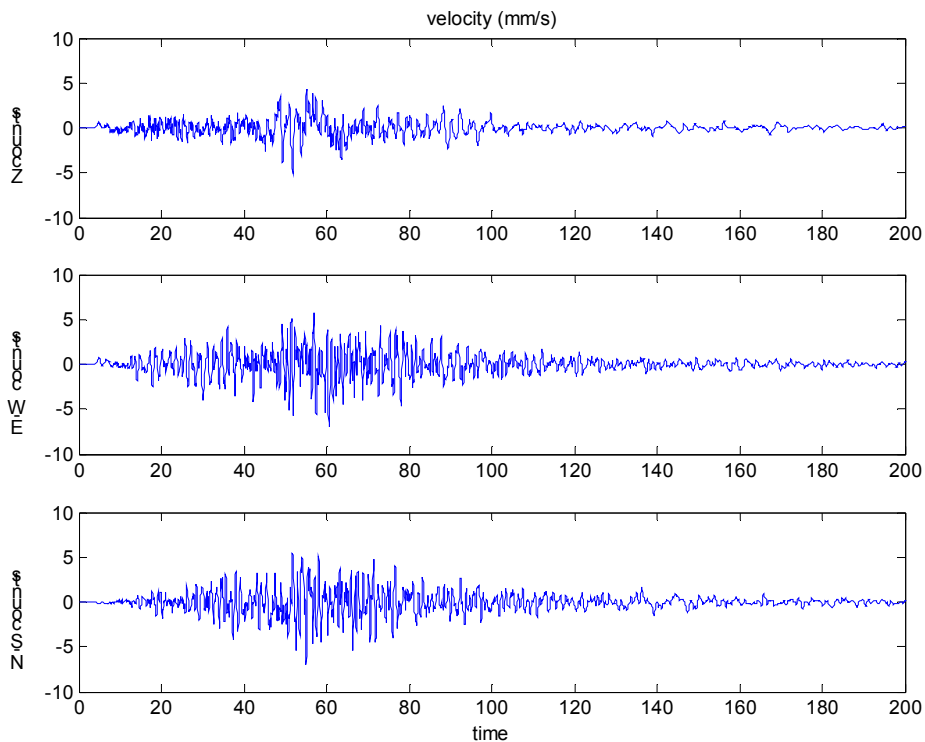


Figure 14: Olympia Earthquake velocity time series [Marka]

The spectrum associated with these data follow in Figure 15.

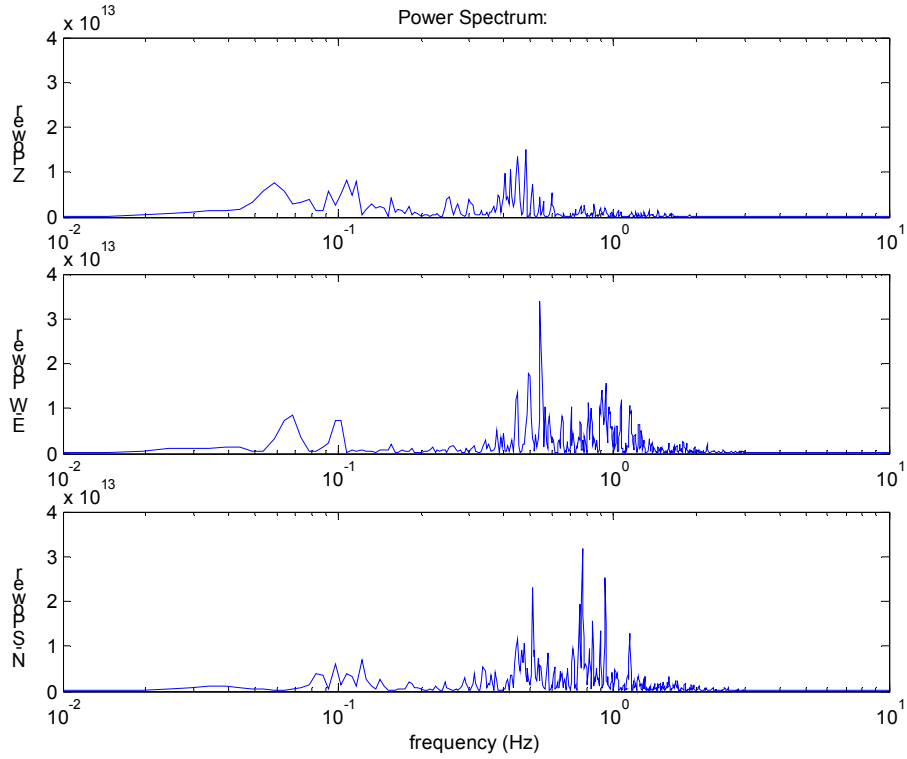


Figure 15: Olympia Earthquake power spectra [Marka]
<http://blue.ligo-wa.caltech.edu/users/robert/samplespectra/allmic.xml>

2.2.5 Impulsive motion

Source	RMS Seismic Amplitude (nm)	Band (Hz)	Approx. Surface Wave Wavelength (m)
Chiller-pad equipment at 100m (water chillers, pumps, air compressors)	0.8	55 to 60	1
Large trucks on Highway 240 at 1.7 km	9	3 to 10	100
Small truck hitting bump in parking lot at 20 mph and 200m	200	5 to 15	30
Otto jumping at 300m	100	5 to 15	30

Table 3: Some impulsive excitation and characteristics, LHO [Schofield]

2.2.6 Identified sources, additional information

2.2.6.1 Seismic wave Q measurements

Figure 16 shows the peak seismic signals at the out-lying stations produced by 3 trucks on Route 240. The Q for the plotted line was calculated from the amplitudes of 7 truck signals recorded at Y-mid and Y-end stations. Maxima in cross correlations between signals from two seismometers set up near Y-end were used to calculate arrival time differences and wavelengths (see <http://www.ligo.caltech.edu/docs/G/G000262-00.pdf>)

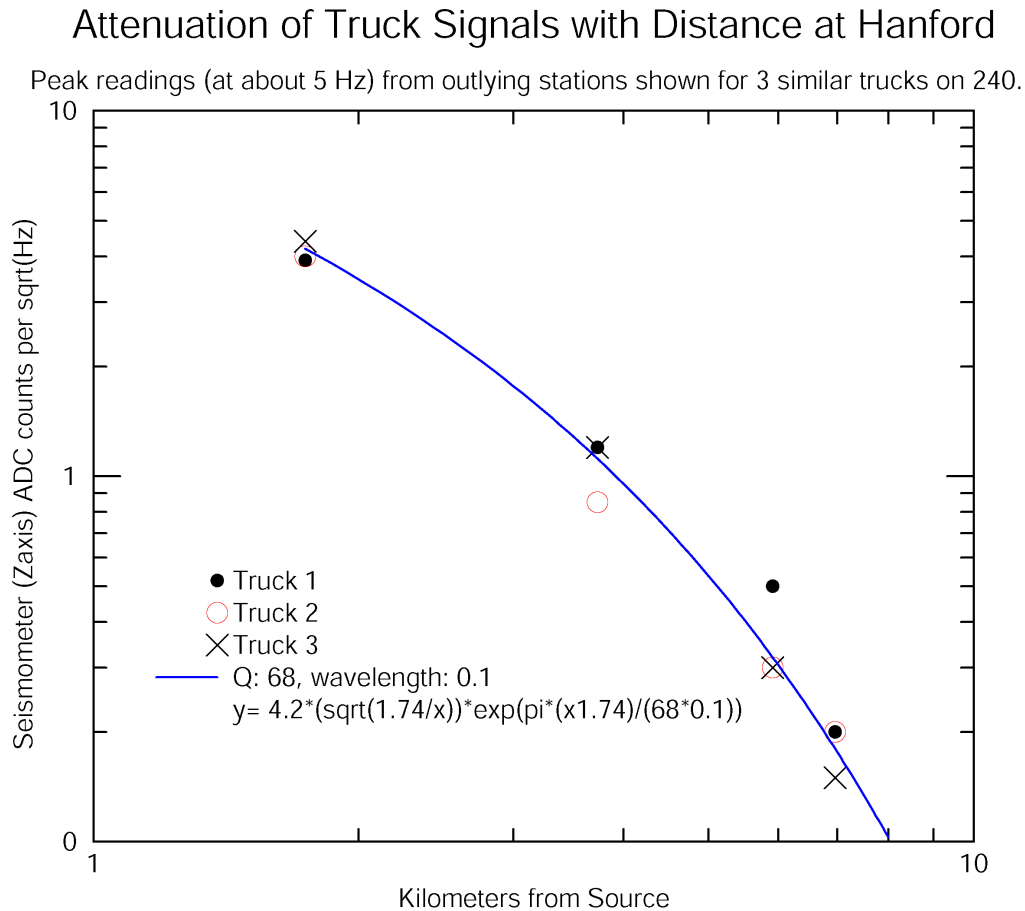


Figure 16: Data and model for attenuation in LHO ground [Schofield]

2.2.6.2 Dispersion measurements

Figure 17 shows a dispersion relation for tamper signals at Hanford. This dispersion relation for tamper vibrations was obtained from the phase difference between signals from 2 separated seismometers near the Y-end at Hanford. Calculated velocities were plotted for frequencies at which the coherence between signals from the two seismometers was greater than 0.99. All stable frequency settings for two different types of tampers were used to maximize the frequency range. Different colors or symbols indicate different runs.

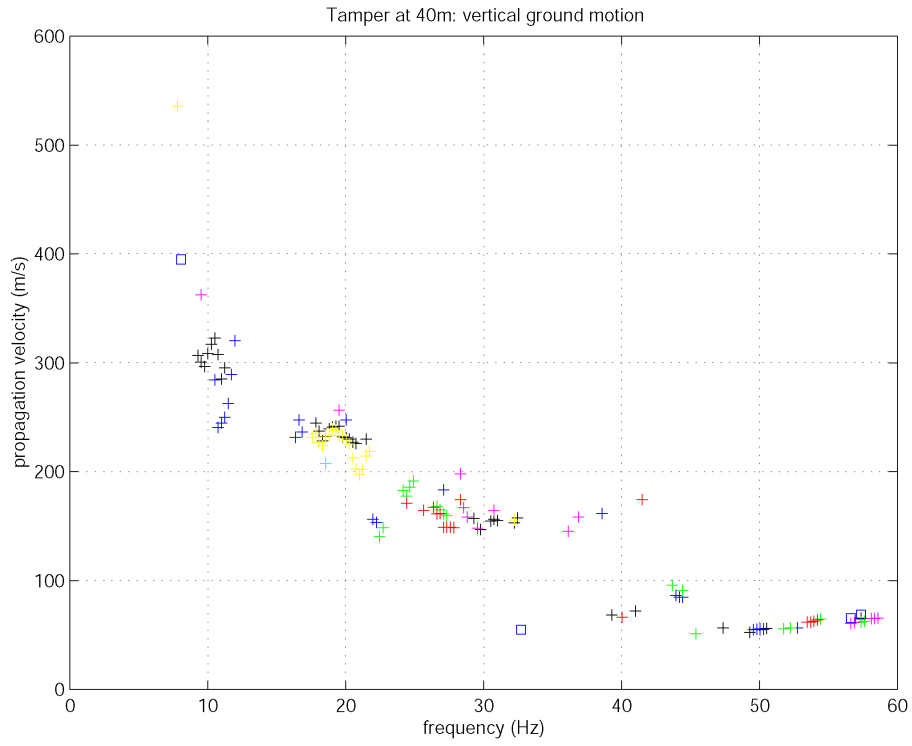


Figure 17: Dispersion of tamper-excited ground motion, LHO [Schofield]

3 Acoustic environment

3.1 Livingston

3.1.1 Spectra, variability

3.1.2 Impulsive events

3.1.3 Identified sources, additional information

3.2 Hanford

3.2.1 Spectra, variability

Power spectral characterization has been performed using the microphones in the vertex (BSC8), Mid-X (BSC5) and Mid-Y (BSC6) stations. The measurements are made under Engineering run operating conditions.

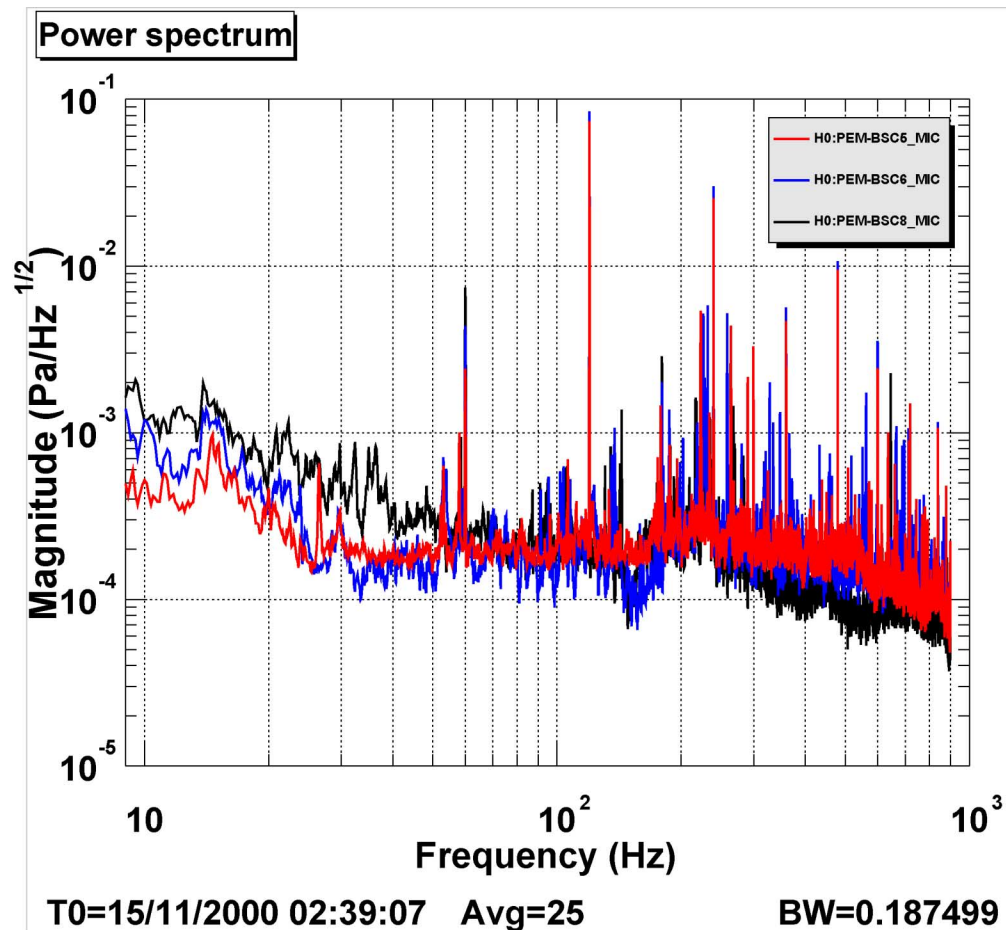


Figure 18: LHO Acoustic spectra, normal operating conditions

3.2.2 Impulsive events

3.2.3 Identified sources, additional information

4 Electromagnetic environment

Initial comparative measurements [Chatterji] for the two sites have been made; see Figure 19. These plots were made outside of the buildings, far from local sources of 60 Hz and multiples. The ‘Reference’ curve is from an earlier measurement (with the low frequencies corrupted by mechanical motion of the coil); it will appear on the figures under LLO and LHO below as a point of reference.

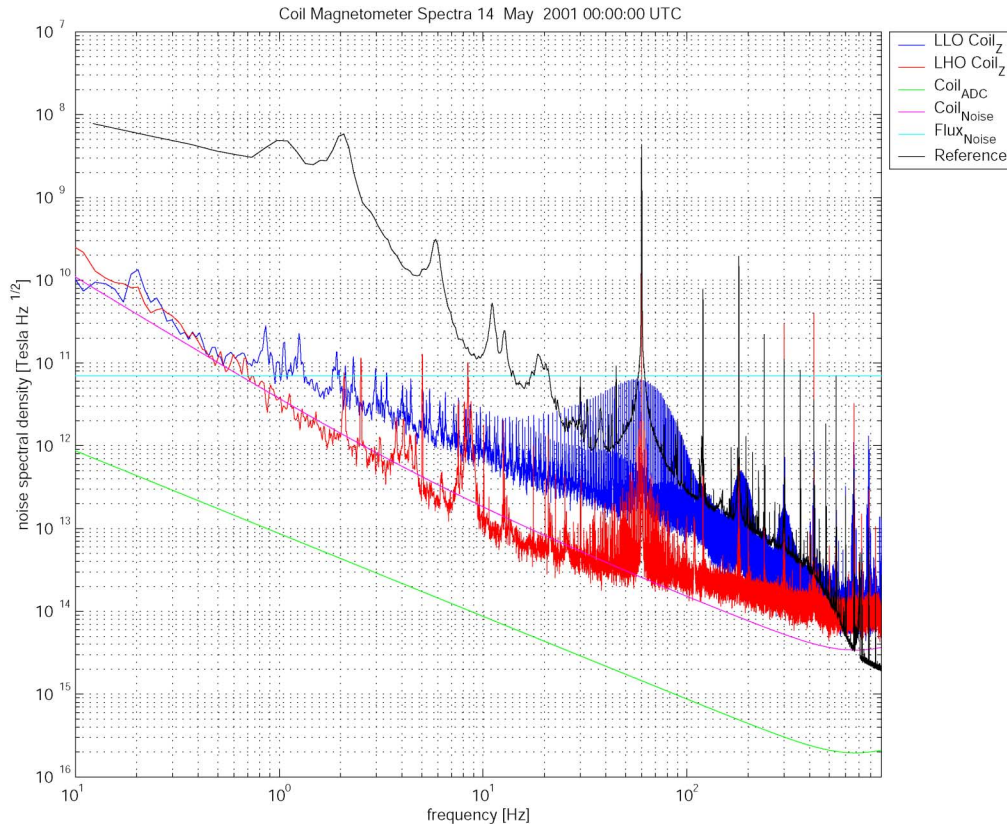


Figure 19: Comparison of LLO and LHO magnetic fields, outside of buildings [Chatterji]

4.1 Livingston

4.1.1 Spectra, variability

High-sensitivity coil magnetometers and the standard flux-gate magnetometers have been put in the LVEA to measure the ambient fields [Chatterji]; the two give similar answers. The flux-gate magnetometers appear to be sensitive enough to make real measurements in that environment; see Figure 20.

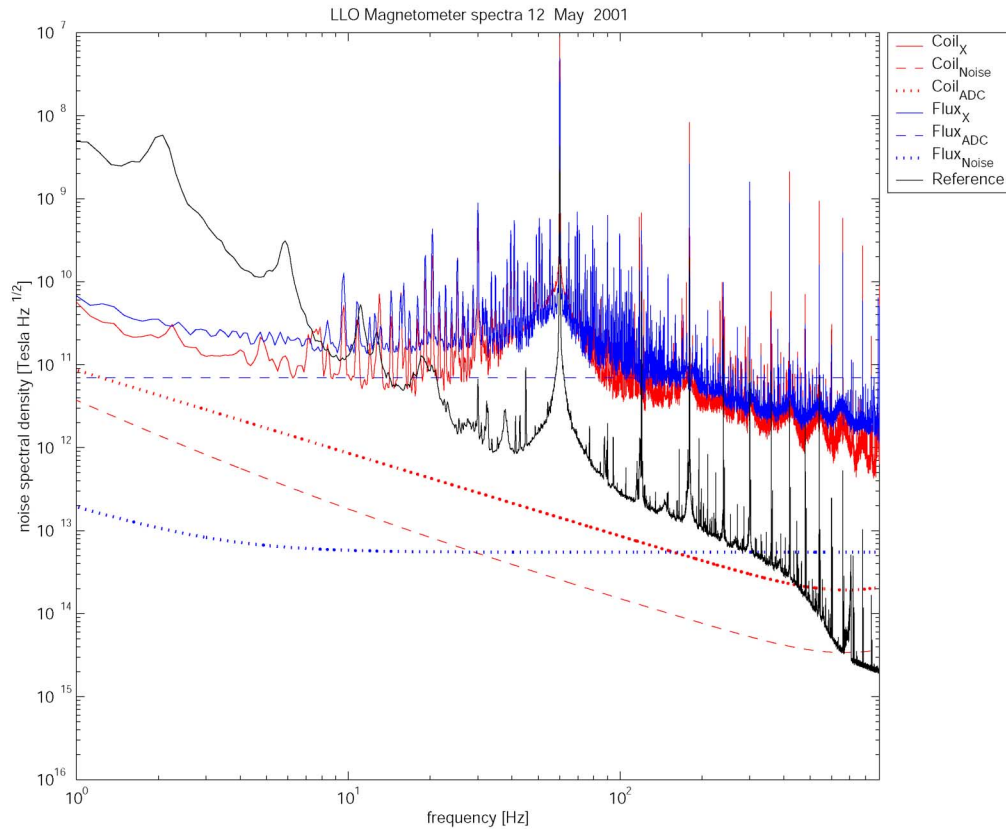


Figure 20: Magnetic fields in the LVEA, LLO [Chatterji]

4.1.2 Impulsive events

4.1.3 Identified sources, additional information

4.2 Hanford

4.2.1 Spectra, variability

4.2.1.1 Magnetic field

Standard flux-gate magnetometers have been put in the x-end station to measure the ambient fields [Chatterji] for the E3, see Figure 21. (The coil data shown should be disregarded; it was not functioning correctly.) Most of the electronic equipment was turned off for this measurement, which may explain the lower noise level, limited by the sensing noise in the flux-gate magnetometer. This plot may be best seen as a measurement of the Bartington flux-gate magnetometer noise floor.

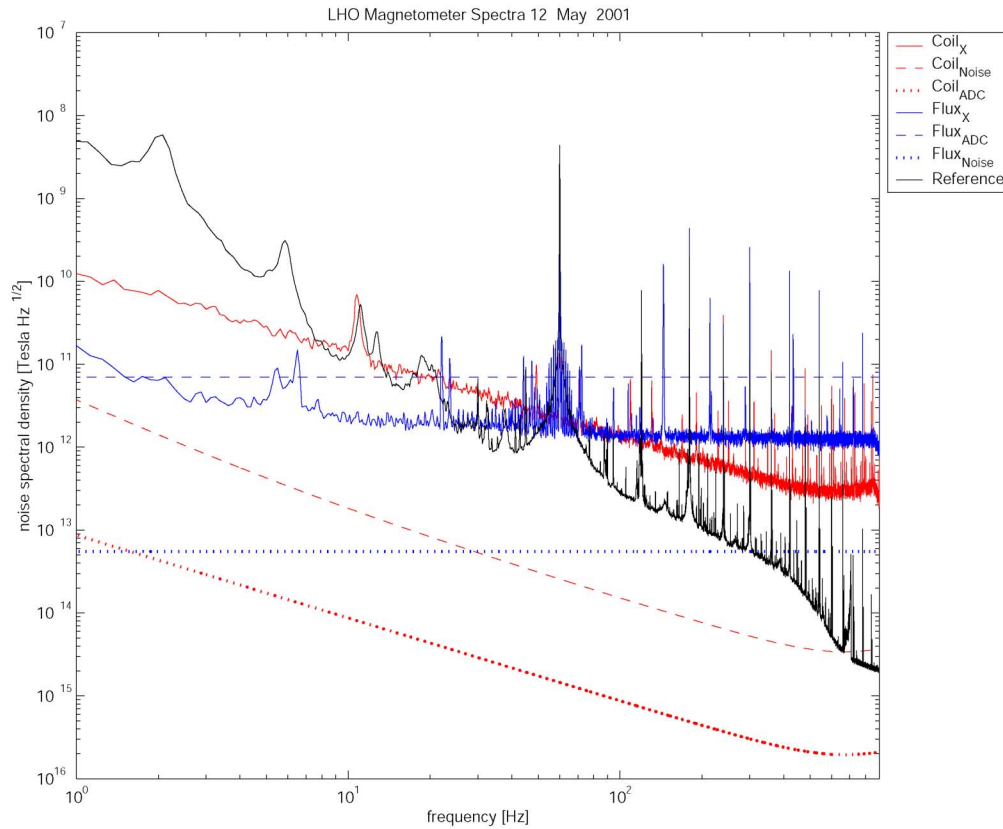


Figure 21: Magnetic field, LHO X-end station. Most electronics turned off [Chatterji]

Additional measurements have been made using the flux-gate instruments; see Figure 22. The specifications show typical noise as about 5 pT at 1 Hz and about 1.5 pT at 10 Hz. It appears that the background is above noise for the low frequencies of the LVEA and perhaps at least 1 of the Mid-Y axes. The broad 60 Hz feature at Mid-Y disappears when the air handler fans are shut off. Judging from the LVEA mag Z, there was a transient during this time series.

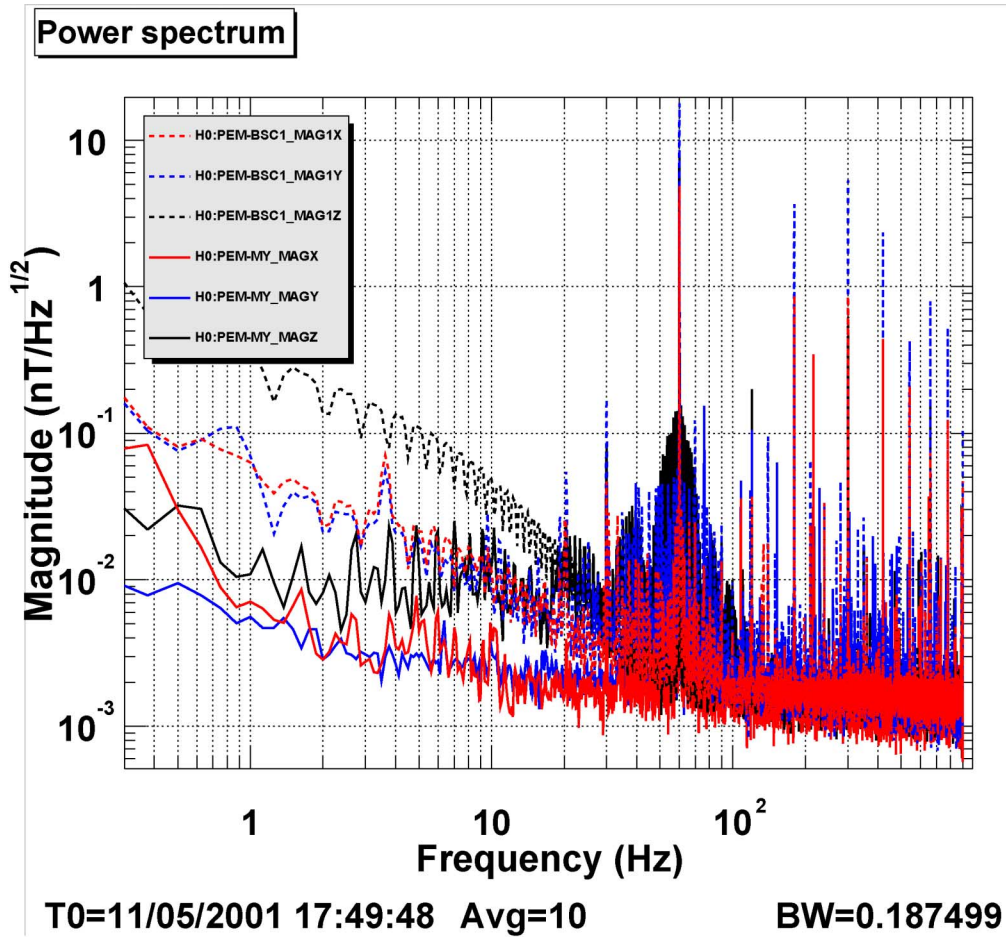


Figure 22: Magnetic field measurements, flux-gate instruments [Schofield]

4.2.2 Impulsive events

4.2.3 Identified sources, additional information

5 Thermal and barometric environment

5.1 Livingston

5.2 Hanford

A year trend for the barometric pressure (and less relevant, the wind speed) is shown in Figure 23.

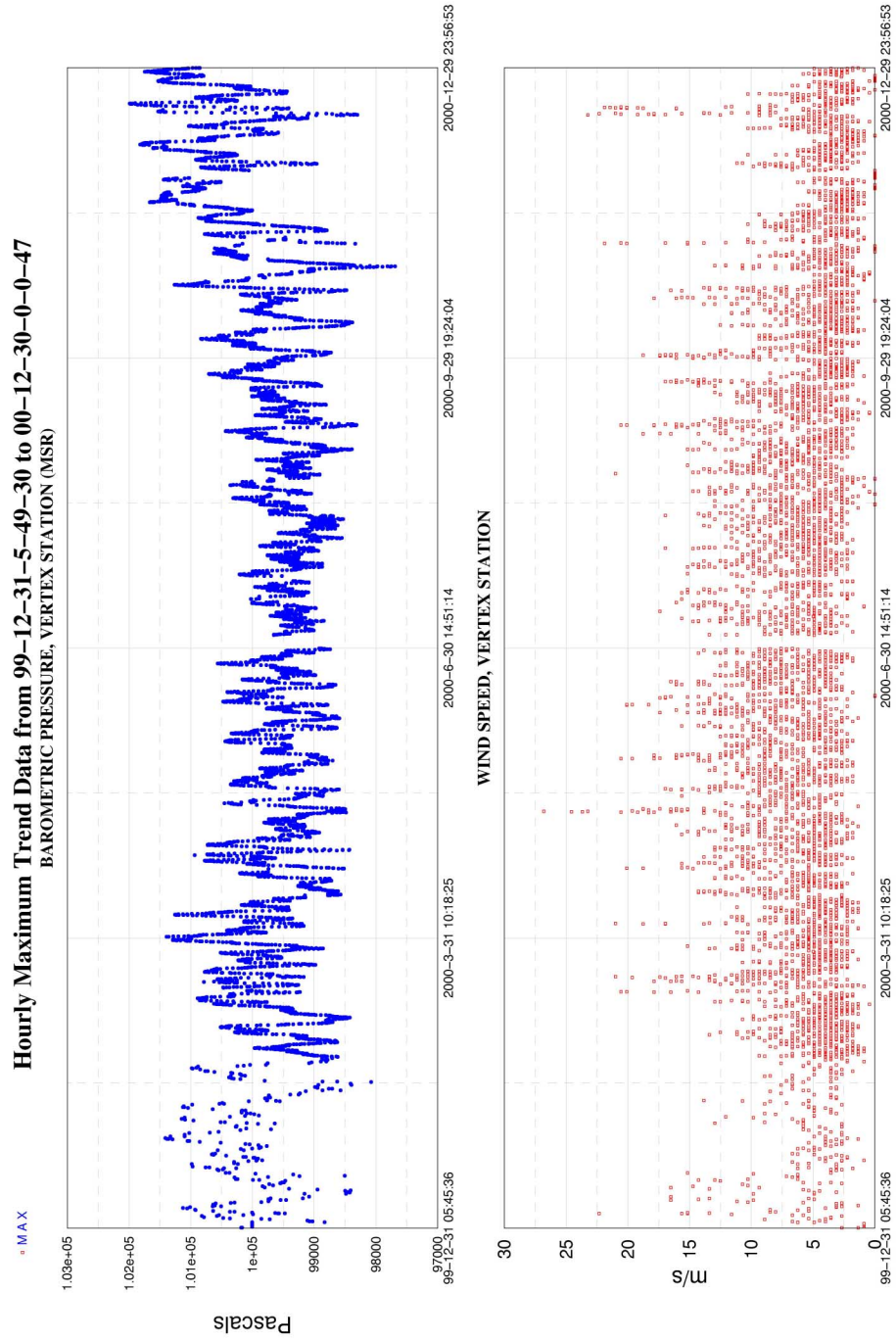


Figure 23: Barometric pressure and windspeed for LHO, year trend

A year trend for the temperature in the LHO LVEA (and outside, less relevant) is shown in Figure 24.

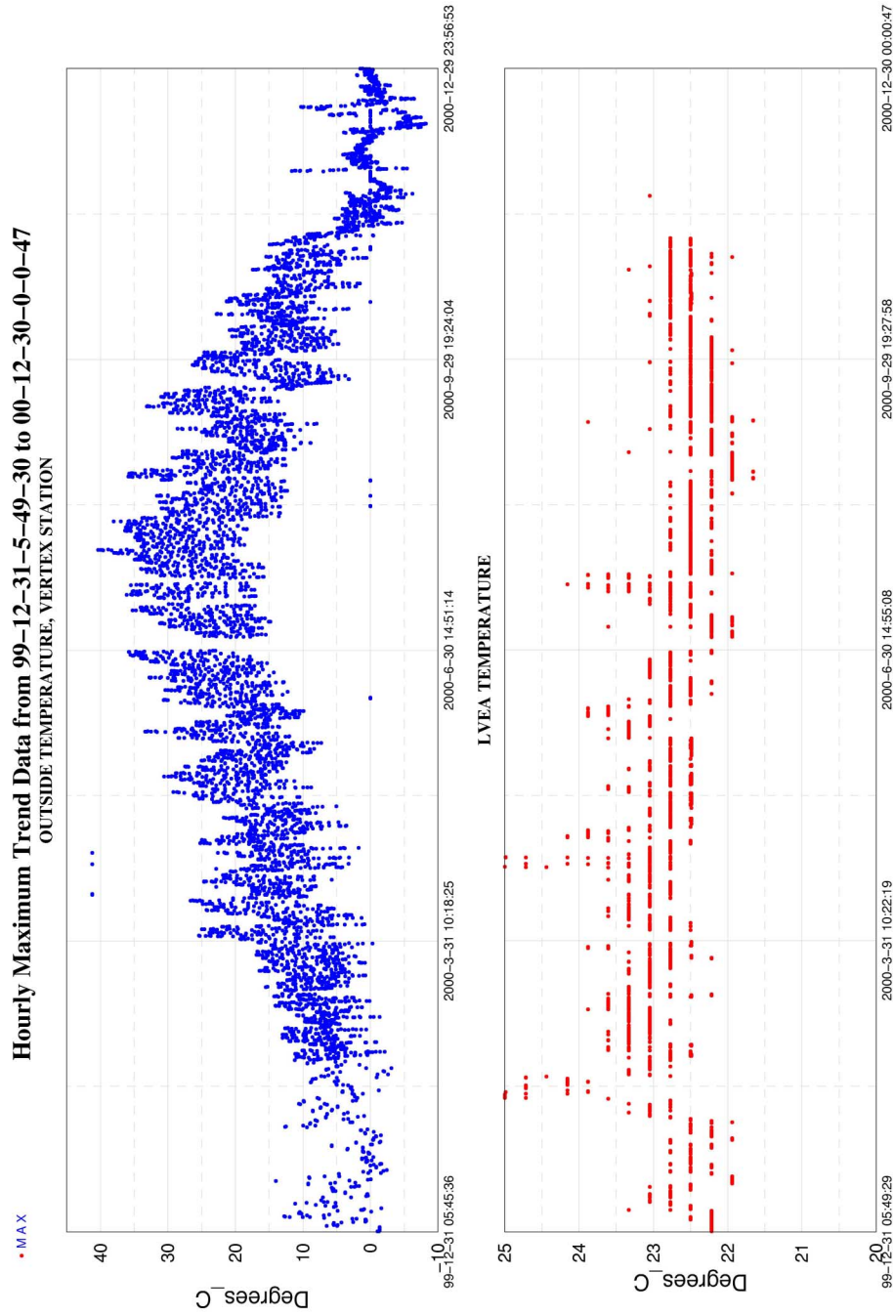


Figure 24: Temperature outside and in the LVEA, LHO, year trend

6 Vacuum environment

The nature and quantity of the residual gas in the beam tubes limits the sensitivity of the interferometers due to statistical variation in the number of gas molecules in the optical path. The measured outgassing rates in a 2km section of installed, baked, beam tube is shown in Table 4: Measured outgassing from Beam Tube, 2km length [Weiss].

2 km module post bake outgassing and leak rate
Outgassing rate of selected gases in torr liters/sec/cm² @ 23 C

molecule	Goal*	HY2	HY1	HX1	HX2	LY2	LY1	LX1	LX2	
H ₂	4.7	4.8	6.3	5.2	4.6	2.6	3.4	6.6	4.3	x10 ⁻¹⁴
CH ₄	4800	< 90	< 22	< 0.9	< 10	< 24	< 3.9	< 3	< 4.0	x10 ⁻¹⁹
H ₂ O	1500	< 4	< 20	< 1.8	< 0.8	< 3	< 0.9	< 0.6	< 10	x10 ⁻¹⁸
CO	650	< 14	< 9	< 5.7	< 2	< 5	< 10	< 8	< 5	x10 ⁻¹⁸
CO ₂	2200	< 40	< 18	< 2.9	< 8.5	< 10	< 6	1.1	< 8	x10 ⁻¹⁹
NO+C ₂ H ₆	7000	< 2	< 14	< 6.6	< 1.0	< 1.9	< 3.6	< 1.1	< 1.1	x10 ⁻¹⁹
H _n C _p O _q	50-2 #	< 15	< 8.5	< 5.3	< 0.4	< 20	< 25	< 1.9	< 4.3	x10 ⁻¹⁹
air leak torr-liters/sec	10	< 2	< 1	< 0.4	< 1.6	< 10	23	< 3.5	< 0.7	x10 ⁻¹⁰

* Goal : maximum outgassing rate to achieve equivalent to 10⁻⁹ torr H₂ with 2000 liter/sec pumps at only stations

Goal for hydrocarbons depends on mass of parent molecule; range corresponds to 100 - 300 AMU

Table 4: Measured outgassing from Beam Tube, 2km length [Weiss]

The anticipated contribution to the equivalent strain sensitivity of an interferometer operating with the measured outgassing, and the initial pumping system, is shown in Figure 25. Additional pumps can be added to lower the noise contribution by about a factor of 10 in strain.

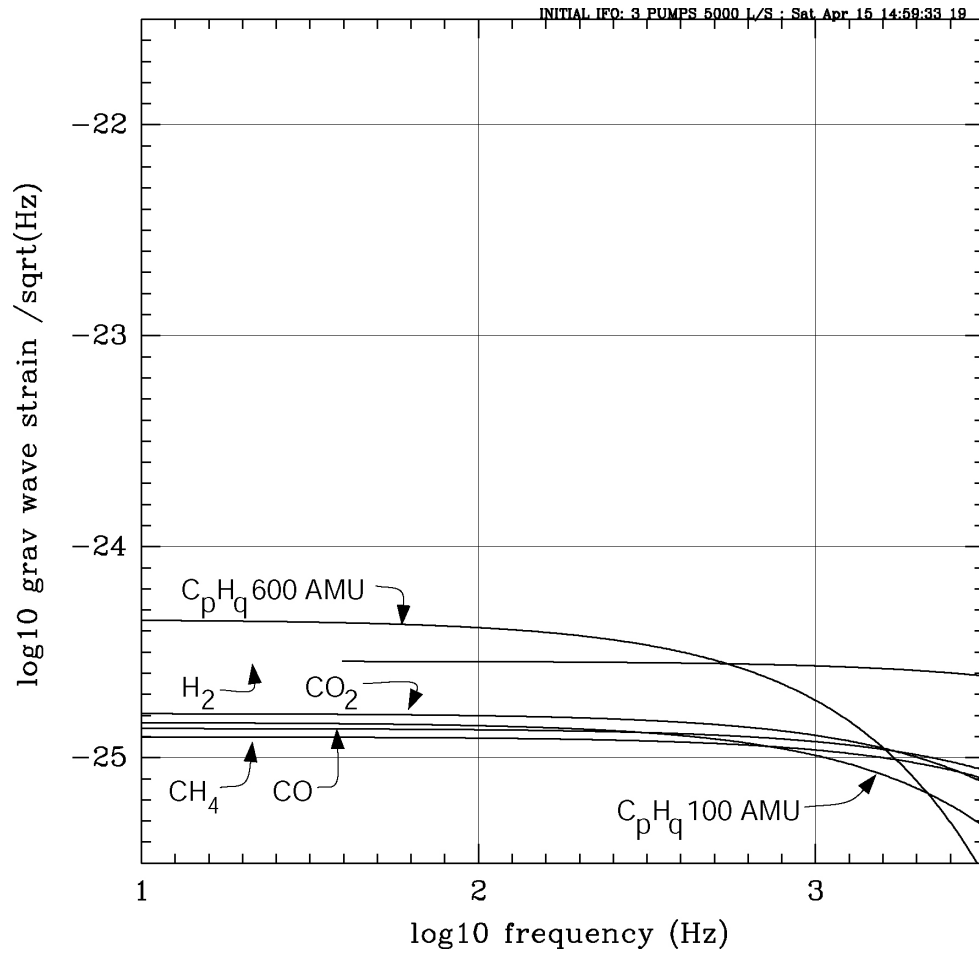


Figure 25: Strain sensitivity as limited by residual gas [Weiss]

6.1 Livingston

6.2 Hanford